Articles

Journal of Avian Biology 47: 263–274, 2016
doi: 10.1111/jav.00826

Subject Editor: Staffan Bensch. Editor-in-Chief: Thomas Alerstam. Accepted 14 September 2015

Shaped by uneven Pleistocene climate: mitochondrial phylogeographic pattern and population history of white wagtail *Motacilla alba* (Aves: Passeriformes)

Xinlei Li, Feng Dong, Fumin Lei, Per Alström, Ruiying Zhang, Anders Ödeen, Jon Fjeldså, Per G. P. Ericson, Fasheng Zou and Xiaojun Yang

X. Li, F. Dong and X. Yang (yangxj@mail.kiz.ac.cn), State Key Laboratory of Genetic Resources and Evolution, Kunming Inst. of Zoology, Chinese Academy of Sciences, Kunming 650223, China. XL also at: Univ. of Chinese Academy of Sciences, Beijing 100049, China. – F. Lei, P. Alström and R. Zhang, Key Laboratory of Zoological Systematics and Evolution, Inst. of Zoology, Chinese Academy of Sciences, Beijing 100101, China. PA also at: Swedish Species Information Centre, Swedish Univ. of Agricultural Sciences, SE-750 07 Uppsala, Sweden. – A. Ödeen, Dept of Animal Ecology, Uppsala Univ., Norbyvägen 18D, SE-752 36 Uppsala, Sweden. – J. Fjeldså, Center for Macroecology, Evolution and Climate, Natural History Museum of Denmark, Univ. of Copenhagen, Universitetsparken 15, DK-2100 Copenhagen, Denmark. – P. G. P. Ericson, Dept of Vertebrate Zoology, Swedish Museum of Natural History, PO Box 50007, SE-10405 Stockholm, Sweden. – F. Zou, South China Inst. of Endangered Animals, Guangzhou 510260, China.

We studied the phylogeography and population history of the white wagtail *Motacilla alba*, which has a vast breeding range, covering areas with different Pleistocene climatic histories. The mitochondrial NADH dehydrogenase subunit II gene (ND2) and Control Region (CR) were analyzed for 273 individuals from 45 localities. Our data comprised all nine subspecies of white wagtail. Four primary clades were inferred (M, N, SW and SE), with indications of *M. grandis* being nested within *M. alba*. The oldest split was between two haplotypes from the endemic Moroccan *M. a. subpersonata* (clade M) and the others, at 0.63–0.96 Mya; other divergences were at 0.31–0.38 Mya. The entire differentiation falls within the part of the Pleistocene characterized by Milankovitch cycles of large amplitudes and durations. Clade N was distributed across the northern Palearctic; clade SW in southwestern Asia plus the British Isles and was predicted by Ecological niche models (ENMs) to occur also in central and south Europe; and clade SE was distributed in central and east Asia. The deep divergence within *M. a. subpersonata* may reflect retention of ancestral haplotypes. Regional differences in historical climates have had different impacts on different populations: clade N expanded after the last glacial maximum (LGM), whereas milder Pleistocene climate of east Asia allowed clade SE a longer expansion time (since MIS 5); clade SW expanded over a similarly long time as clade SE, which is untypical for European species. ENMs supported these conclusions in that the northern part of the Eurasian continent was unsuitable during the LGM, whereas southern parts remained suitable. The recent divergences and poor structure in the mitochondrial tree contrasts strongly with the pronounced, well defined phenotypical differentiation, indicating extremely fast plumage divergence.

The phylogeographic structure of species or groups of closely related species have often been explained from prominent climatic oscillations during the Pleistocene, which have had profound impacts on phylogeographic patterns of contemporary species (Hewitt 1996, 2000, 2004, Avise 2009). Comprehensive phylogeographic studies in Europe have confirmed how species distributions became fragmented and restricted to refugial areas during the last glacial maximum (LGM) (Hewitt 1996, 2000). While northern Europe and North America were covered by large ice sheets during the LGM, northern Asia had permafrost but limited amounts of ice-sheets (Williams et al. 1998). Modelling based on pollen records by Allen et al. (2010) indicated that the woody vegetation (trees and shrubs) of northern Asia had shrunk towards the south during the LGM, although much of Siberia had a vegetation of mesophilous herbs, often referred to as the 'mammoth steppe'. Several studies have shown that many bird species contain clades with present northern distributions that went through population growth, and these clades are often widespread (Pavlova et al. 2006, Zink et al. 2006, 2008, Haring et al. 2007, Saitoh et al. 2010, Zhao et al. 2012). Meanwhile, east Asia (here referring mainly to China, the Korean peninsula Japan and Mongolia) was less affected by glaciation except in the higher mountains (Williams et al. 1998). During the LGM, temperatures of east Asia were higher than in Europe and North America at similar latitudes, and permafrost existed only at high elevations (Weaver et al. 1998, Williams et al. 1998, Otto-Bliesner et al. 2006). Reconstructions of the palaeo-vegetation of east Asia have also indicated that a diverse flora existed during the LGM, especially in the southern part (Harrison et al. 2001). Analyses of east Asian birds have indicated that most studied

species in this region possessed a prominent phylogeographic structure, and that they expanded before the LGM (Li et al. 2009, Song et al. 2009, Huang et al. 2010, Dai et al. 2011, Qu et al. 2012, Zhao et al. 2012, Dong et al. 2013, Wang et al. 2013). The Mediterranean Basin was little affected by glaciation (Weaver et al. 1998, Otto-Bliesner et al. 2006), and harbored important glacial refugia, and has been identified as a hot spot in terms of speciation events (Guillaumet et al. 2006, García et al. 2008, Hourlay et al. 2008, Pons et al. 2011, Stervander et al. 2015).

The white wagtail *Motacilla alba* has a vast breeding range, covering the northwesternmost corner of Africa (Morocco), all of Europe and the temperate parts of Asia to western Alaska (Alström et al. 2003, del Hoyo et al. 2004). Northern populations are long distance migrants, whereas southern populations are short distance migrants or resident (Alström et al. 2003, del Hoyo et al. 2004). The white wagtail is a very adaptable species, occurring in a variety of open habitats from sea level to high elevations (up to ~ 5000 m), usually near water bodies, and often close to or within human habitation (Alström et al. 2003, del Hoyo et al. 2004). There is pronounced plumage variation within the white wagtail, and Alström et al. (2003) recognized nine distinct subspecies. Although the white wagtail is usually treated as a polytypic species (Alström et al. 2003, del Hoyo et al. 2004, Dickinson and Christidis 2014, Gill and Donsker 2015), especially the taxa *personata* and *lugens* (Stepanyan 1990), and sometimes all nine morphologically distinct taxa (Avibase 2015), have been treated as specifically distinct.

Pavlova et al. (2005) analyzed mitochondrial DNA and plumage from seven of the nine subspecies (*alba*, *baicalensis*, *ocularis*, *lugens*, *personata, leucopsis* and *alboides*, the last one only mentioned briefly in 'Note in proof'), mainly from Russia, and found three main clades: 1) a widespread clade containing representatives from six of the studied subspecies (excluding *alboides*); 2) a clade with samples from Almaty in Kazakhstan (*M. a. personata*), Vietnam (*M. a. alboides*) and southeast Russia (Primor'e; subspecies *leucopsis*, one sample of *M. a. lugens*); and 3) a clade from Krasnodar in the Caucasus region (*M. a. alba*). There was no phylogeographic structure within any of these clades, except for separation between Almaty and Primor'e samples in the second clade, and none of the subspecies was inferred to be reciprocally monophyletic. Pavlova et al. (2005) suggested that these three clades had survived glacial times in the Far East, the Caspian-Caucasus area and lower latitude Asian regions, respectively, and recently come into contact at Primor'e and Krasnodar. Especially the widespread northern clade was estimated to have gone through a recent population expansion (Pavlova et al. 2005).

The sampling of Pavlova et al. (2005) was focused on northern populations, whereas the southern part of the breeding range of the white wagtail, which had milder Pleistocene climates, may have had different population histories. The aim of this paper is to increase the sampling effort of Pavlova et al. (2005) to include southern areas and all nine subspecies, which would help to better understand the phylogeographic structure and population history of the white wagtail.

Material and methods

Sampling

We focused on sampling from the southern part of the range of the white wagtail, and a total of 50 individuals from 16 localities were collected. Tissue samples were stored in pure alcohol at –80°C. Sequences were also obtained from a few toepad samples form museum specimens. We also downloaded mitochondrial sequences of 223 individuals from GenBank. The sample localities are shown in Fig. 1, and details (museum/collection number, taxon, type of tissue, etc.) of all samples are included in Supplementary material Appendix 1.

Most of the individuals we sampled were considered to be on their breeding grounds, sampled during June to early August, or from locally breeding subspecies. Ten individuals from Zunyi (Guizhou Province, China), two individuals from Nuristan Province (Afghanistan) and one individual from Fujian Province (China) were sampled ahead of this period (in May), knowing that white wagtails start to breed early in those parts (Peng et al. 1987, Zhao 2001). Moreover, four individuals from Nei Mongol Autonomous Region (China) sampled on 6 September, two individuals from the Kuriles sampled in April and one individual from Jutland (Denmark) sampled in late August were included. The sequences downloaded from GenBank, from Pavlova et al. (2005), were from individuals collected on the breeding grounds, as stated in that paper.

Taxonomy follows Alström et al. (2003).

Laboratory procedure

The lab work was done in three different labs, the Kunming Inst. of Zoology, China, the Swedish Museum of Natural History, Stockholm, Sweden, and Uppsala Univ., Uppsala, Sweden, here refered to as procedure 1, 2 and 3, respectively. Polymerase chain reaction (PCR) was used to amplify partial or comeplete NADH dehydrogenase subunit II gene (ND2) and partial or comeplete Control Region (CR) sequence of mitochondrial DNA. Sequences of all the primers are given in Supplementary material Appendix 2.

Procedure 1: the tissues were treated with SDS Lysis Buffer, Potassium Acetate and then isopropanol to precipitate gross DNA. Partial ND2 was amplified using two pairs of primers: L5219 (Sorenson et al. 1999) and H5880 (Dong et al. 2010); L5809 (Cicero and Johnson 2001, modified) and H6312 (Cicero and Johnson 2001, modified). PCR amplification was carried out in a total volume of 20 µl, with an initial denaturation at 94°C for 5 min, then 40 cycles of 94°C for 30 s, 50°C for 40 s and 72°C for 60 s, a final extension at 72°C for 7 min completed the reaction. The primers LCR4 (Tarr 1995) and LCON2 (Zink and Blackwell 1998) were used to amplify CR sequence with the same total volume. PCR conditions of CR were similar to those described by Pavlova et al. (2005). PCR products were sequenced with the same primers used for amplification. The PCR products were purified using a SanPrep Column DNA Gel Extraction Kit (Sangon Biotech) and sequenced with the BigDye Terminator sequencing Cycle Sequencing Kits on an ABI 3730xl Analyzer.

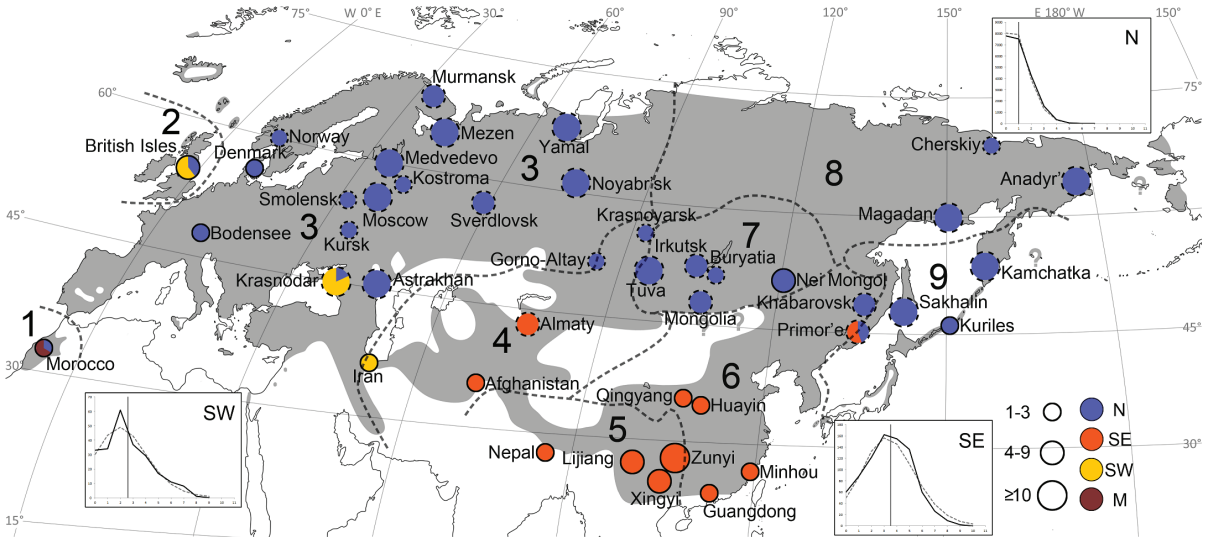

Figure 1. Phylogeographic structure and mismatch distribution of the white wagtail. Grey area indicates breeding range (from Alström et al. 2003). Our sample localities are represented by solid circles and previous sample localities by dashed circles. Blue, red, yellow and brown circles indicate clade N, SE, SW and M in Fig. 2, respectively. Mismatch distributions of three clades are shown: solid line represents observed value, dashed line indicates model distribution, and vertical line indicates mean number of differences. Numbers 1–9 indicate subspecies separated by dashed lines based on Alström et al. (2003): 1, *M. a. subpersonata*; 2, *M. a. yarrellii*; 3, *M. a. alba*; 4, *M. a. personata*; 5, *M. a. alboides*; 6, *M. a. leucopsis*; 7, *M. a. baicalensis*; 8, *M. a. ocularis*; 9, *M. a. lugens*.

Procedure 2: toepads were softened in double distilled water, and then the gross DNA was extracted using the DNeasy Tissue kit (Qiagen, Hilden, Germany). Partial ND2 and CR ware both amplified with multiple pairs of primers designed for this study. ND2: MAL_ND2_F1 and MAL_ND2_R1, MAL_ND2_F2 and MAL_ND2_R2N, MAL_ND2_F3 and MAL_ND2_R3, MAL_ND2_F4 and MAL_ND2_R4, MAL_ND2_F5 and MAL_ND2_R5. CR: MAL_CR_F1 and MAL_CR_R1, MAL_CR_F2 and MAL_CR_R2, MAL_CR_F3 and MAL_CR_R3. PCR amplification of ND2 was carried out in a total volume of 25 µl with an initial denaturation at 94°C for 5 min, followed by 2 cycles of 30 s at 94°C, 30 s at 56°C and 30 s at 72°C, and then the annealing temperature was decreased to 54°C and 52°C in the next two cycles, the finally 34 cycles were performed with an annealing temperature of 50°C; the final extension lasted for 7 min at 72°C. The PCR amplification of CR was carried out in a same total volume, and the amplification protocol was similar to that of ND2, only the annealing temperature in each steps were decreased by 2°C. PCR products were sequenced with the same primers used for amplification. The PCR products were purified using a QIAquick PCR purification kit (Qiagen) and the sequencing using the BigDye Terminator method on an ABI 3730xl Analyzer.

Procedure 3: two mtDNA fragments were sequenced: the complete ND2, and a segment comprising the complete or partial CR with or without partial tRNA-Pro, the NADH dehydrogenase subunit VI gene (ND6) and tRNA-Glu flanking the 5′ end of CR, plus the complete tRNA-Phe and part of the 12S ribosomal RNA gene. DNA was extracted from blood, muscle tissue and feathers using the DNeasy Tissue Kit (Qiagen). PCR primer pair for ND2 was L5215 (Hackett 1996) and H6313 (Johnson and Sorenson 1998). Three pairs were used for the CR: FCRI5′ (Boag in Baker and Marshall 1997) and F389 (Baker and Marshall 1997) or L16150 (Saetre et al. 2001) and F389, and F304 (Baker and Marshall 1997) and H1343 (Berg et al. 1995). PCR amplifications were carried out in 25-µl volumes. The PCR cycle for ND2 involved an initial 3 min denaturation at 94°C, followed by 38 cycles of 15 s denaturation at 94°C, 15 s annealing at 51°C and 45 s extension at 72°C and ending with a 2 min extension step at 72°C. The PCR cycle for CR was 3 min at 94°C, 35 cycles of 15 s at 94°C, 30 s at 63°C and 1 min at 72°C, plus a final 10 min at 72°C. Gel electrophoresis in 2% agarose was performed on 5 µl of each PCR product to affirm length and specificity of the amplifications and the remaining 20 µl was typically purified with Microcon PCR and YM-100 Centrifugal Filter Devices (Millipore). The purified products were cycle sequenced with the primers L5215, L5758M (Ödeen and Björklund 2003), H5776 (Klicka et al. 2000), H5950 (Ödeen and Björklund 2003), H6313 (ND2), APC1 (Ödeen and Björklund 2003), F304, F389, FCRI5′, L16576, L16749 and MCRI2 (Ödeen and Björklund 2003) (CR), usually with the BigDye Terminator Ready Reaction kit (Applied Biosystems) and run on ABI-prism 310 and 377 automated sequencers. Some PCR product was purified with ExoSAP-IT (Affymetrix USB) and sequenced externally by Macrogen (South Korea).

Population structure analyses

Sequencing results were visualized and assembled in SeqMan (DNASTAR). Sequence alignment was done in Clustal X (Thompson et al. 1997). All sequences were modified to the same length and ambiguous sites were completely deleted from the alignment. The final length of partial ND2 and CR were 917 bp and 360 bp respectively. All sequences have been deposited in GenBank (accession numbers KT031286–KT031385, Supplementary material Appendix 1). Because

mitochondrial genes belong to the same linkage group, the two markers were combined in all analyses.

We built haplotype maximum likelihood (ML) and Bayesian inference (BI) trees to infer the population structure of the white wagtail. Three close relatives of the white wagtail (Ödeen and Alström 2001, Alström and Ödeen 2002) were selected as outgroups: Japanese wagtail *M. grandis*, white-browed wagtail *M. maderaspatensis* and African pied wagtail *M. aguimp* (Supplementary material Appendix 1). The optimal substitution model for the concatenated dataset was GTR+G, which was selected in jModeltest 0.1.1 (Guindon and Gascuel 2003, Posada 2008) by the Akaike information criterion (AIC) (Posada and Buckley 2004). Rate variation across sites was accounted for using a discrete gamma distribution. ML analyses were carried out using PhyML 3.0 (Guindon and Gascuel 2003). Search strategy was set as best of NNI and SPR, and reliability of each node was estimated through non-parametric bootstrapping (100 replicates). BI analyses were carried out using MrBayes 3.1.2 (Ronquist and Huelsenbeck 2003). As per default, three hot and one cold chains were used. MCMCs was set to eight million generations and sampled every 1000 generations. Two parallel runs were performed and convergence was checked in Tracer ver. 1.4.1 (Rambaut and Drummond 2007). Default priors were used. The first 25% samples were discarded as 'burn-in'. Support values were represented by posterior probabilities (PP).

A maximum parsimony network was constructed in TCS ver. 1.12 (Clement et al. 2000) to better visualize the genetic structure of the white wagtail. Connection limit was set to 95% as default. The output was edited in yED Graph Editor 3.9 (yWorks 2012) to generate the final graph. Genetic distances between populations were calculated in MEGA 5.05 (Tamura et al. 2011) using the Kimura 2-Parameter (K2P) model (Kimura 1980). The K2P model was selected because it is an often used model in population genetics studies, despite that it was not the best-fit model for the dataset, but genetic distances were also calculated under the JC69 and HKY models as well as uncorrected distances (not shown), and the differences between these were extremely slight. In other respects, the recommendations by Fregin et al. (2012) for calculating genetic distances were followed, i.e. using perfectly homologous sequences (same length, same part of locus) and completely delete uncertain nucleotides.

Molecular clock calibration

Most calibrations of the avian mitochondrial molecular clock have been done for the cytochrome b gene (cyt-b) (Lovette 2004, Weir and Schluter 2008). The cyt-b clock has been estimated to have an average rate of 2.1% (±0.1%, 95% CI) divergence/million years (Weir and Schluter 2008). The molecular clock of ND2 has been found to vary among taxa (Lerner et al. 2011, Manthey et al. 2011), and CR sequences have an even greater rate of variation (Zink and Blackwell 1998, Ruokonen and Kvist 2002, Drovetski 2003, Zink and Weckstein 2003). For these reasons, a calibration was deemed necessary for the molecular clock rate of combined ND2 and CR sequences of the white wagtail.

First, we calibrated the partial ND2 clock rate of the genus *Motacilla*. The full cyt-b and ND2 sequences of 29 individuals from 9 species of *Motacilla* were downloaded from GenBank (Supplementary material Appendix 1). The ND2 sequences from GenBank were trimmed to the same length and section as our ND2 sequences. The ratio between average within-genus distance of cyt-b and ND2 was calculated, then multiplied by the cyt-b clock rate 2.1% to get the partial ND2 rate of *Motacilla*, i.e. 3.02%/million years. Second, we assumed that the partial ND2 clock rate of white wagtail was the same as that rate of *Motacilla* (3.02%/million years). Then we calculated the intraspecies average distances of the white wagtail using concatenated sequences and partial ND2 sequences separately (all sequences of the white wagtail were involved). The ratio of these two distances was multiplied by the partial ND2 clock rate (3.02%) to get the clock rate of the concatenated sequences. The resulting rate was 2.7% (0.0135 substitutions/site/million years).

Diversification time estimate

Diversification time was estimated in BEAST ver. 1.8.0 (Drummond et al. 2012). Groups were defined based on the results from population structure analyses in order to estimate the time to the most recent common ancestor (TMRCA). The optimal substitution model was selected by jModeltest (GTR+G). Lognormal relaxed clock (uncorrelated) was used in order to consider rate variation among clades. The molecular clock rate was fixed to 0.0135 substitutions/site/ ineage/million years, as calculated. Different analyses were run using different tree priors: Coalescent – Expansion Growth; Speciation – Birth-Death Process; and Speciation – Yule Process. In the prior panel, the initial value and mean value of alpha was set to 0.128 as estimated by jModeltest. The MCMC chain was run for 100 million generations and sampled every 2000 generations. The resulting log file was analyzed in Tracer ver. 1.4.1 to ascertain that the analysis had converged (when ESS > 200 and the trace of parameters had stabilized).

Genetic diversity and historical demography

Nucleotide diversity (π), haplotype diversity (h) and number of polymorphic sites (S) were calculated in DnaSP ver. 5 (Librado and Rozas 2009). Tajima' *D* test (Tajima 1989) and Fu's *Fs* test (Fu 1997) were performed in Arlequin 3.5 (Excoffier and Lischer 2010) to examine whether a population departed from a mutation-drift equilibrium, significance judged by 25 000 simulated samples. A significantly negative value is often taken as an indicator of population expansion.

We implemented Bayesian Skyline Plot (BSP) in BEAST ver. 1.8.0 (Drummond et al. 2012) to estimate changes in effective population size since TMRCA. The substitution model was selected by jModeltest 0.1.1 (Guindon and Gascuel 2003, Posada 2008). A lognormal relaxed uncorrelated clock was set with the same clock rate as above, and with Coalescent: Bayesian Skyline selected. The beginning and mean values of parameter alpha were also set as estimated by jModeltest 0.1.1. A MCMC chain was run for 100 million generations and sampled every 2000 generations. Convergence was checked in Tracer ver. 1.4.1 (Rambaut and Drummond 2007). After convergence was confirmed,

a graph of BSP was generated in Tracer with the first 20% samples discarded as 'burn-in'.

In addition to BSP, mismatch distribution was calculated in Arlequin 3.5 (Excoffier and Lischer 2010). A Mismatch distribution calculates the distribution of pairwise differences. Unimodal distribution often indicates recent population expansion and the closer the peak to the y axis, the more recently the expansion has happened (Rogers and Harpending 1992). The sum of square deviations (SSD) between the observed and the expected mismatch was calculated, and a significant SSD value means the observed value does not fit sudden expansion model. Performance of expansion parameters was tested with 10 000 bootstrap replicates, and genetic distance was set to pairwise difference. Time of expansion (t) could be drawn from the parameter τ and equation $\tau = 2\mu kt$, where k is the number of nucleotides and μ is the mutation rate of combined sequence (1.35%/lineage/million years).

Ecological niche models (ENMs)

The ENMs aim to find associations between the known occurrence of a species and environmental variables, and then apply the association to forecast distribution of this species under different climatic conditions (Martinez-Meyer and Peterson 2006). This method is controversial because it relies on the assumption that ecological niche evolution is conservative (Guisan and Thuiller 2005). Some existing studies have proved the conservativeness of ecological niches (Peterson et al. 1999, Martinez-Meyer and Peterson 2006), and this method has been widely used in avian phylogeographic studies to verify the impact of Pleistocene ice ages (Walstrom et al. 2012, Wang et al. 2013, Qu et al. 2014). We used ENMs to compare the simulated present and LGM distribution of the white wagtail, which would help understanding the impact of the Pleistocene ice ages.

Occurrence data was obtained from the publicly available database Global Biodiversity Information Facility (GBIF, <http://data.gbif.org>), which includes a number of museum specimen databases (e.g. ORNIS, <www.ornisnet.org>). Specimen records were used preferentially when performing ENMs. All repeated or closely clustered records (<3.5 km) and non-breeding period records were eliminated. Occurrence data with 'has Geospatial Issues' were also excluded. The occurrence data were heavily biased, as more than 90% of the records were from Europe. Two procedures were taken to handle this bias: first, we calculated the density of records in areas with little data, and then we randomly sampled records at over-sampled areas to balance the overall density of records. The imbalanced distribution of occurrence data might represent the actual distribution of the white wagtail to some degree, but this information was decreased after the procedures above. However, as the white wagtail is a highly adaptable species (Alström et al. 2003, del Hoyo et al. 2004), the uneven observation effort rather than natural population density is most likely the cause of the paucity of records in the eastern part of the range. Second, we created a bias file to handle the deficiency of occurrence data in especially central and east Russia. The areas without records were weighted by 0, other areas by 1.

Nineteen environmental layers (bio1–bio19) of current and LGM at 2.5 arc-minutes resolution were downloaded from WorldClim website (<www.worldclim.org>) (Hijmans et al. 2005). Climate layers of LGM were generated from Community Climate System Model 4 (CCSM 4). We used ENMTools (Warren et al. 2010) to calculate the Pearson's correlation coefficient between environmental variables. Highly correlated variables were removed until no pairwise correlation coefficient was greater than 0.8. Final modeling included 8 variables (bio 2, bio 5–8, bio 12, bio 14 and bio 15).

ENMs were performed in MaxEnt ver. 3.3.3 (Phillips and Dudik 2008) because MaxEnt has been shown to yield robust results even for sparsely sampled data (Pearson et al. 2007). Random seed and subsample were selected to enable a random test. Twenty percent occurrence data was used to test model performance. The model was run for 15 times with maximum iterations set to 2000, allowing the model to have adequate time to converge. A bias file described above was imported to minimize sampling bias. The resulting ASCII file was converted to raster and reclassified in ArcGIS 9.3 (ESRI) for applying the 10 percentile training presence logistic threshold to define minimum probability of suitable habitats.

Results

Phylogeographic structure

The ML and BI trees based on concatenated sequences showed similar topologies (Fig. 2). Both trees inferred the white wagtail to be paraphyletic since *M. grandis* was sister to all white wagtail subspecies except two *M. a. subpersonata* (clade M), although the lack of support (node B) rendered the tree effectively trichotomous in this respect. The parsimony haplotype networks showed that *M. grandis* and clade M were separated from the others by a minimum of 29 and 26 steps, respectively, while the smallest distances among the others were five steps between clades N and SW, six steps between clades N and SE and 11 steps between clades SW and SE (Fig. 3). Both the gene trees and haplotype networks indicated that the remaining white wagtails formed three primary clades (Fig. 2, Fig. 3): north (N), representing *M. a. alba*, *M. a. baicalensis*, *M. a. ocularis*, *M. a. lugens* and *M. a. personata*, as well as a minor part of the samples of *M. a. yarrellii*, *M. a. leucopsis* and a single *M. a. subpersonata*; southeast (SE) representing *M. a. personata*, *M. a. alboides* and *M. a. leucopsis* and a minor part of the samples of *M. a. lugens*; and southwest (SW), representing *M. a. alba* and three of the five samples of *M. a. yarrellii*. The two aberrant *M. a. subpersonata* haplotypes from Morocco in clade M (node A) were 2.3% divergent from the other white wagtails, whereas the genetic divergences among clades N, SE and SW were 0.4%. The SE and N clades were identified as sisters, although this was unsupported (PP 0.76; bootstrap 26%, node D). The oldest split, betwen clade M and the other white wagtails (node A), was estimated at 0.63–0.96 million yr ago (Mya), i.e. around the junction of middle and early Pleistocene. The divergence of clades SE, N and SW (node C) at 0.37–0.39 Mya and the separation of clades SE and N at 0.31–0.33 Mya (node D) were within the middle Pleistocene (Table 1). As the phylogenetic relationships between clades N, SE and SW did not get high nodal

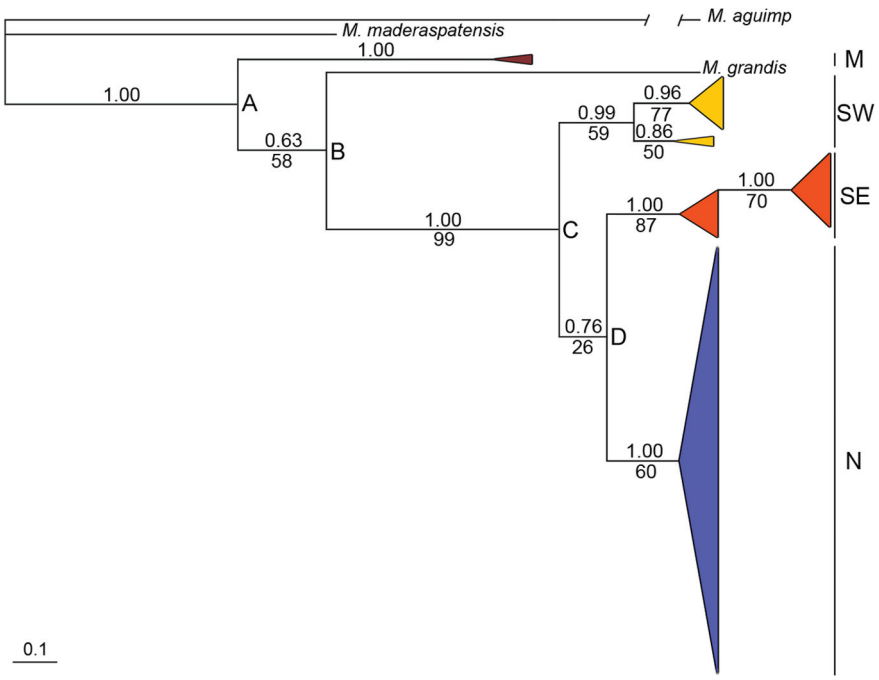

Figure 2. Tree based on concatenated ND2 and CR, inferred by Bayesian inference. Posterior probabilities are shown above the branches and maximum likelihood bootstrap values below the branches. Northern clade (N), south-eastern clade (SE), south-western clade (SW) and Moroccan clade (M) were represented by blue, red, yellow and brown respectively. Main nodes are indicated with capital letters A, B, C and D.

support (node D), the corresponding splitting times should be considered as tentative.

The geographic distribution of the clades is shown in Fig. 1. Clade N was distributed across the northern part of the species' range, with a single sample from Morocco (from the endemic *M. a. subpersonata*). Representatives for clade SW were found at three localities (Caspian–Black Sea area and the British Isles). Clade SE, which was mainly distributed in east Asia and central Asia, was subdivided into two clades, but neither of these corresponded to a geographical area or subspecies, and accordingly there was no phylogeographic structure within this clade.

Genetic diversity

We obtained 917 bp of ND2 and 360 bp of CR sequences for 273 samples. Seventy nine haplotypes of ND2 were defined by 89 polymorphic sites (39 singletons, 50 parsimony informative sites), and 25 haplotypes of CR were defined by 31 polymorphic sites (18 singletons, 13 parsimony informative sites). For combined sequences, 95 haplotypes were defined by 120 polymorphic sites (57 singletons, 63 parsimony informative sites). Overall haplotype diversity was 0.788 and overall nucleotide diversity was 0.00387. The genetic diversity of each clade is shown in Table 2. Excluding clade M, for which only two samples were available, clade SE had the highest haplotype diversity and nucleotide diversity, while clade N had the lowest values. The nucleotide diversity of clade N was very low, about an order of magnitudes lower than that of the two other clades. The commonest haplotype in clade N was shared by 60% of the individuals in that clade, occupying 28 out of 32 sampling localities of clade N.

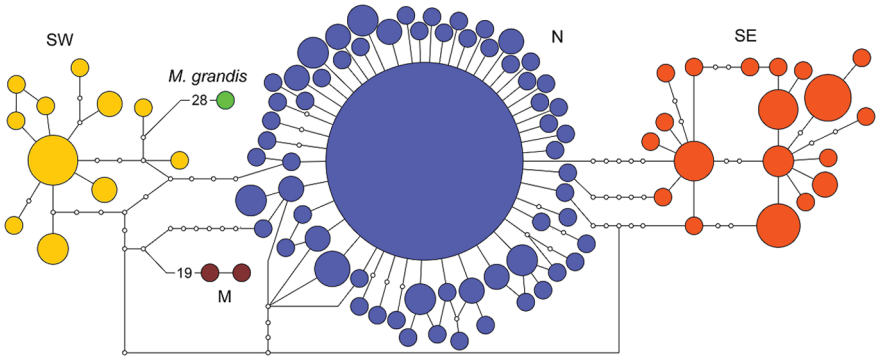

Figure 3. Parsimony haplotype network of white wagtail and *M. grandis*. Different colours represent clades in accordance with Fig. 2, and *M. grandis* was represented by green. Each colored circle represents a haplotype, and the area of a circle is proportional to the number of individuals with this haplotype. Small, unfilled circles represent missing haplotypes. Clade M and *M. grandis* are relatively distant from other white wagtails, and the associated numbers indicate the amount of missing haplotypes.

Table 1. Divergence time estimation of the white wagtail. The unit is in million years. The 95% HPD is shown in brackets.

TMRCA	M–SE, N, SW	SE, N–SW	SE–N
Expansion growth	0.96 (0.62–1.33)	0.37 (0.24–0.52)	0.31 (0.19–0.45)
Birth-death process	0.66 (0.39–0.93)	0.39 (0.26–0.52)	0.33 (0.22–0.46)
Yule process	0.63 (0.38–0.89)	0.38 (0.26–0.51)	0.33 (0.22–0.45)

Table 2. Diversity indicators and expansion time (by mismatch distribution) of each clade. *p < 0.05, **p < 0.01.

	n	h	Hd	π	Peak	SSD	Tajima' *D*	Fu's *Fs*	τ	Expansion (years ago)
SE	41	19	0.927	0.00263	unimodal	0.00208	–1.15770	–8.95897**	3.86523	112 000 (56 000–156 000)
SW	22	11	0.857	0.00203	unimodal	0.00541	–1.62681*	–4.16682*	2.29102	66 000 (24 000–150 000)
N	208	63	0.639	0.00081	unimodal	0.00091	–2.73935**	–29.78464**	0.98438	29 000 (22 000–37 000)

Historical demography

According to the BSP, clades SE and SW both began to expand about 0.1 Mya, during the Marine Isotope Stage (MIS) 5 when the climate was relatively warm (Fig. 4). Effective population size of clade SE grew slowly until a rapid increase about 30 000 yr ago, while the SW clade kept growing slowly until it reached equilibrium about 40 000 yr ago. BSP analysis of clade N failed to converge, probably due to the very shallow divergence within this clade (60% of the individuals of this clade belonged to the same haplotype).

The mismatch distributions for clades SE, SW and N were unimodal and did not deviate from a model of demographic expansion, supporting that these clades went through sudden population expansions (Fig. 1; Table 2; clade M not tested due to small sample). The expansion time of clade SE estimated by mismatch distribution was consistent with that estimated by the BSP, whereas the expansion time of clade SW estimated by mismatch distribution was later (66 000 yr ago, 95% HPD 24 000–150 000 yr ago) but still before MIS 2. Expansion time of clade N estimated by τ was 29 000 years ago (95% HPD 22 000–37 000 yr ago) during MIS 2, about LGM.

Tajima' *D* and Fu's *Fs* test of clades SE, SW and N all showed significant negative values except Tajima's *D* value for clade SE (Table 2), further indicating past population expansion of these three clades (clade M not tested due to small sample).

Ecological niche models

The distribution estimated by ENMs under present climate is consistent with the actual breeding range of the white wagtail except for some of the most northern breeding areas, which were estimated to be unsuitable (Fig. 5). Nevertheless, The ENMs indicated that the range of the white wagtail shrunk heavily in the north during the LGM. On the other hand, broad areas where clade SE and SW are distributed at present remained suitable for the white wagtail during the LGM.

Discussion

Phylogeographic structure and effects of Pleistocene climates

The mitochondrial haplotypes of the white wagtail were divided into four primary clades, with *M. grandis* nested within *M. alba* (though without statistical support). These

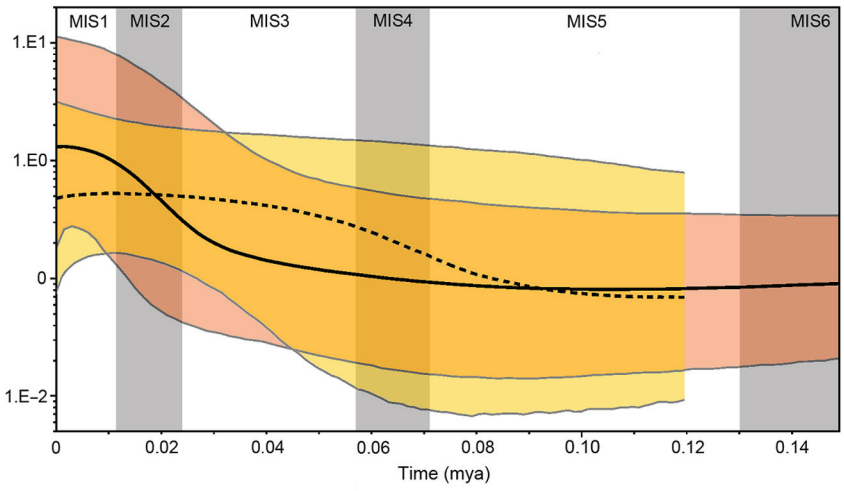

Figure 4. Bayesian skyline plot (BSP) of clade SE (solid line and red background) and clade SW (dashed line and yellow background). The x axis represents a time scale in units of million years ago and the y axis represents N_{ef}. The central lines show mean N_{ef} and the colored backgrounds define the 95% HPD limits. The grey vertical bars indicate cold period marine isotope stages (MIS).

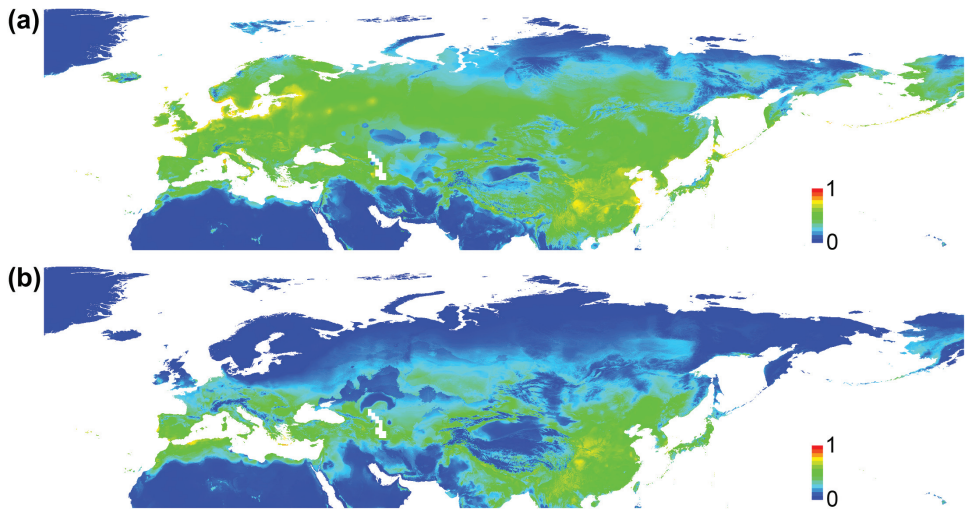

Figure 5. Ecological niche models of the white wagtail (AUC = 0.744). (a) Present; (b) LGM. Different colors mean different probability of occurrence; green indicates conditions typical of those where the species is found.

four clades represent different geographical regions, with evidence of incomplete lineage sorting and/or introgression. Within these four primary clades we failed to find any genetic sub-structure and the divergences among clades N, SW and SE were shallow and only dating back to the middle Pleistocene. The entire mitochondrial history of the white wagtail falls within the last 960 000 yr, a period characterized by large-amplitude Milankovitch oscillations, which should select for increased vagility and generalism (cf. Dynesius and Jansson 2000). The lack of structure and shallow divergence in clade N might have been caused by strong post-LGM population expansions into previously uncolonized regions. Evidence from mismatch distribution, very low nucleotide diversity, highly significant Tajima' *D* and Fu's *Fs* test values and star-like network all indicate that clade N went through a dramatic recent population expansion. This is in agreement with several previous studies from the Palearctic (Pavlova et al. 2006, Zink et al. 2006, 2008, Haring et al. 2007, Saitoh et al. 2010, Zhao et al. 2012) and North America (Klicka et al. 2011, Smith et al. 2011, van Els et al. 2012). The post-LGM expansion of clade N is also supported by the ENMs which indicate that most of the present distribution of clade N was not suitable habitat for the white wagtail during the LGM. The white wagtail breeds north to 73°N at present (Alström et al. 2003), but during the LGM, it was restricted to about 55°N in Asia and about 50°N in Europe according to the ENMs. In contrast, the lack of structure in especially clade SE is at odds with most studies of birds from that region (Li et al. 2009, Song et al. 2009, Huang et al. 2010, Dai et al. 2011, Qu et al. 2012, Zhao et al. 2012, Dong et al. 2013, Wang et al. 2013). However, unlike the white wagtail, these are resident forest birds, which occur at least partly in mountainous regions where climatic oscillations may have fragmented their ranges and thereby promoted divergence. The white wagtail occurs in open, fairly homogeneous habitats, is highly adaptable and evidently has great capacity for long-distance movements, so it is less likely than these resident forest-dwelling species to become geographically fragmented. Most low altitude regions of east Asia remained suitable during the LGM for the white wagtail as shown by ENMs.

More data are needed to establish the distribution of the SW clade. Pavlova et al. (2005) found it exclusively in Krasnodar in the Caucasus region, but we encountered it also in Iran (both these *M. a. alba*) and, surprisingly, in the British Isles (*M. a. yarrellii*). The results of the ENMs indicated that there was broad continuous suitable habitat in the southern part of Europe and west Asia during the LGM, excluding high altitude parts of mountain regions (e.g. the Alps and the Dinara Mountains). It can be hypothesized that clade SW rather than clade N had a range extending from Iran across southern Europe during the LGM, because clade N had shrunk heavily at that time. Due to the lack of samples from the Mediterranean region, it is not possible to tell whether clade SW is still present across southern Europe or whether it may have been replaced by the expanding haplotype group N, resulting in a relictual distribution of clade SW.

In agreement with Pavlova et al. (2005), our results suggest that all three white wagtail clades went through population expansion and only mixed at the edges of their distributions relatively recently. Three of the main clades have experienced different population histories influenced by different historical climates. The climate of the northern Palearctic was severe during the LGM, and did not allow clade N to expand until after the LGM. Relatively mild LGM climate in east Asia enabled clade SE to expand pre-LGM during the interglacial period MIS5, as has been noted in other east Asian birds (Li et al. 2009, Song et al. 2009, Huang et al. 2010, Dai et al. 2011, Qu et al. 2012, Zhao et al. 2012, Dong et al. 2013, Wang et al. 2013). The SW clade also had a pre-LGM expansion during MIS5, which may be untypical for European species (Hewitt 2000, 2004, Brito 2005, Zhao et al. 2012). The strong adaptability of white wagtail may have enabled this species to retain a large population size during MIS2.

It is unlikely that multiple refugia existed for clade N because we detected no divergence within this clade. Refugia of clade N might have been in the Far Eastern part of Eurasia as discussed by Pavlova et al. (2005) and for other

birds by Saitoh et al. (2010). Clade SW might have survived the LGM south of the Black Sea (Pavlova et al. 2005) or even in southern Europe where climate was suitable during LGM. Preliminary data showed that clade SE might have survived earlier glacial periods in southern China as one population (Zunyi) did not show population expansion as revealed by mismatch distribution (another nearby population of Xingyi showed population expansion, but it is likely that some related individuals were sampled here) (Supplementary material Appendix 3).

The polytypic yellow wagtail *Motacilla flava* complex occupies almost the same breeding range as the white wagtail, though it is absent from the southern part of east Asia (Alström et al. 2003). The yellow wagtail has been suggested to be paraphyletic with respect to the citrine wagtail *M. citreola*, and to have a deep genetic split between eastern and western populations (Ödeen 2001, Ödeen and Alström 2001, Alström and Ödeen 2002, Voelker 2002, Alström et al. 2003, Ödeen and Björklund 2003, Pavlova et al. 2003), unlike in the white wagtail. Ödeen and Björklund (2003) studied the western Palearctic clade of yellow wagtail, and showed that in common with the white wagtail this clade had been isolated in glacial refugia and gone through postglacial colonization. Southern subspecies of the western clade, which breed around the Mediterranean, showed no evidence of recent population expansion (Ödeen and Björklund 2003), which may indicate a similar population history to the white wagtail clade SW, which showed an old expansion.

Weir and Schluter (2004) analyzed a number of boreal North American forest 'superspecies' and concluded that all coalesced during the Pleistocene, in agreement with the situation for the white wagtail taxa. In contrast, Saitoh et al. (2010) noted that a number of clades of northeastern Palearctic birds diversified during the Pliocene, and suggested that this might have been due to longer survival of eastern Palearctic clades as a result of less severe conditions in that region compared to northern North America.

Aberrant haplotype divergence in *M. a. subpersonata*

The deep divergence within the endemic, locally distributed and rare Moroccan subspecies *M. a. subpersonata* is remarkable, and is similar to that between other white wagtails and *M. grandis*. The three individuals were identified by plumage, excluding the possibility of the bird with a northern haplotype being a migrant *M. a. alba*. There are at least three alternative explanations for the observed pattern. The aberrant haplotype is 1) the result of introgression from an extinct taxon; 2) it may represent an 'original' haplotype in *M. a. subpersonata*, in which case the N clade haplotype is the result of introgression; or 3) it represents an accidentally amplified nuclear copy, a 'numt' (Sorenson and Quinn 1998). Several facts indicate that the mtDNA PCR products are indeed of mitochondrial origin, and not nuclear copies: 1) no unexpected stop codons or frameshift mutations were present in the coding genes. 2) Direct PCR was performed on as long fragments as possible (often 2 kb, including regions adjacent to the target loci) to reduce the risk of accidental amplification of numts (Sorenson and Quinn 1998). 3) Trees based on the independently amplified mtDNA fragments (not shown) were not in conflict with each other, which is unlikely if one or more of the data sets consists of mixed mtDNA and numts. 4) Overlapping parts of sequences produced by different primers were identical. It is unlikely that several primer combinations would preferentially amplify a numt. 5) Blood and feathers from the same individual gave identical sequences. Accidental amplification of numts is less likely from feathers than from blood (Sorenson and Quinn 1998). Deep divergences have recently been discovered in common redstart *Phoenicurus phoenicurus* (Johnsen et al. 2010, Hogner et al. 2012) and northern raven *Corvus corax* (Webb et al. 2011), and in these cases, the authors suggested that the anomalous pattern probably resulted from ancient secondary contact and interbreeding between divergent populations, and this seems to be the most plausible explanation also for the situation in *M. a. subpersonata*. Northwest Africa holds a number of endemic taxa, which shows the importance of this area for speciation (Guillaumet et al. 2006, García et al. 2008, Hourlay et al. 2008, Pons et al. 2011, Stervander et al. 2015).

Incongruence between plumage divergence and mitochondrial DNA

The shallow mitochondrial divergence and poor geographic structure in mtDNA in the white wagtail stands in stark contrast to the pronounced plumage divergence among the nine subspecies (cf. Alström et al. 2003). This pattern suggests either 1) recent origin, with the plumages evolving considerably faster than the sorting of the mtDNA haplotypes, as has been suggested for the white wagtail (Pavlova et al. 2005), or 2) introgression and homogenization of mtDNA through a selective sweep, as has been suggested for some other birds (Alström et al. 2008, Irwin et al. 2009, Wang et al. 2014; see Rheindt and Edwards 2011). Recent origin is supported by the distributional pattern, with all taxa having parapatric breeding ranges and interbreeding in contact zones (Alström et al. 2003). Although there is evidence of recent introgression, e.g. between *M. a. leucopsis* and *M. a. lugens* and between *M. a. personata* and *M. a. alba/baicalensis*, as already shown by Pavlova et al. (2005), it seems unlikely that a selective sweep could have affected the entire population that is spread out over such a vast area, with highly different environmental conditions among different regions (cf. Rheindt and Edwards 2011). More data are needed to test this. At any rate, the striking plumage differences between the different taxa (Alström et al. 2003) suggest periods of independent evolution in geographically separated areas.

Conclusions

The oscillating Pleistocene climate has strongly influenced the phylogeographic pattern and population history of the white wagtail, although the very high adaptability and vagility of this species has weakened the influence to some extent. The prominent phenotypic differentiation, manifested by the nine distinct subspecies, has most probably evolved extremely fast, within the Pleistocene, with mitochondrial divergence lagging behind; four primary mitochondrial clades showed very slight divergences, with no substructure within, and only one clade was restricted to a

single subspecies (the Moroccan endemic *M. a. subpersonata*). The present study does not provide any new evidence in support of recognition of some of the taxa as separate species, but more research is needed on especially the Moroccan endemic *M. a. subpersonata*. Future studies combining mitochondrial and nuclear markers or using next-generation sequencing techinques will help further elucidate the phylogeographic processes of the white wagtail.

Acknowledgements – Many thanks to Ting Li, Anders Lindström, Ulf Johansson, Rong Yang, Mingwang Zhang, Aiwu Jiang, Yapeng Zhao, Shuwei Liu and Fei Wu for sampling assistance, and to Pierre-André Crochet and Alban Guillaumet for a sample of *M. a. subpersonata*. Thanks are also due to Mengyin An and Martin Irestedt for help in the laboratory. This work was supported by a Major International (Regional) Joint Research Project (no. 31010103901 to FL, XY, PA, JF and PGP), the National Science Fund for Distinguished Young Scientists (no. 31101636, to FD); the Chinese Academy of Sciences Visiting Professorship for Senior International Scientists (no. 2011T2S04) and the Sound Approach (both to PA), and the Swedish Research Council (no. 621-2013-5161 to PE).

References

Allen, J. R. M., Hickler, T., Singarayer, J. S., Sykes, M. T., Valdes, P. J. and Huntley, B. 2010. Last glacial vegetation of northern Eurasia. – Quat. Sci. Rev. 29: 2604–2618.

Alström, P. and Ödeen, A. 2002. Incongruence between mitochondrial DNA, nuclear DNA and non-molecular data in the avian genus *Motacilla*: implications for estimates of species phylogenies. – PhD thesis, Uppsala Univ.

Alström, P., Mild, K. and Zetterstrom, B. 2003. Pipits and wagtials of Europe, Asia and North America: identification and systematics. – Princeton Univ. Press.

Alström, P., Olsson, U., Lei, F. M., Wang, H.-T., Gao, W. and Sundberg, P. 2008. Phylogeny and classification of the Old World Emberizini (Aves, Passeriformes). – Mol. Phylogenet. Evol. 47: 960–973.

Avibase 2015. – <http://avibase.bsc-eoc.org>.

Avise, J. C. 2009. Phylogeography: retrospect and prospect. – J. Biogeogr. 36: 3–15.

Baker, A. J. and Marshall, D. H. 1997. Mitochondrial control region sequences as tools for understanding evolution. – In: Mindell, D. P. (ed.), Avian molecular evolution and systematics. Academic Press, pp. 51–82.

Berg, T., Moum, T. and Johansen, S. 1995. Variable numbers of simple tandem repeats make birds of the order Ciconiiformes heteroplasmic in their mitochondrial genomes. – Curr. Genet. 27: 257–262.

Brito, P. H. 2005. The influence of Pleistocene glacial refugia on tawny owl genetic diversity and phylogeography in western Europe. – Mol. Ecol. 14: 3077–3094.

Cicero, C. and Johnson, N. K. 2001. Higher-level phylogeny of new world vireos (Aves: Vireonidae) based on sequences of multiple mitochondrial DNA genes. – Mol. Phylogenet. Evol. 20: 27–40.

Clement, M., Posada, D. and Crandall, K. A. 2000. TCS: a computer program to estimate gene genealogies. – Mol. Ecol. 9: 1657–1659.

Dai, C. Y., Zhao, N., Wang, W. J., Lin, C. T., Gao, B., Yang, X. J., Zhang, Z. W. and Lei, F. M. 2011. Profound climatic effects on two east Asian black-throated tits (Ave: Aegithalidae), revealed by ecological niche models and phylogeographic analysis. – PLoS One 6: e29329.

del Hoyo, J., Elliott, A. and Christie, D. A. 2004. Handbook of the birds of the world. Vol. 9. Cotingas to pipits and wagtails. – Lynx Edicions.

Dickinson, E. and Christidis, L. 2014. The Howard and Moore complete checklist of the birds of the world, 4th ed. Vol. 2: Passerines. – Aves Press.

Dong, F., Wu, F., Liu, L. M. and Yang, X. J. 2010. Molecular phylogeny of the barwings (Ayes: Timaliidae: *Actinodura*), a paraphyletic group, and its taxonomic implications. – Zool. Stud. 49: 703–709.

Dong, L., Heckel, G., Liang, W. and Zhang, Y. Y. 2013. Phylogeography of silver pheasant (*Lophura nycthemera* L.) across China: aggregate effects of refugia, introgression and riverine barriers. – Mol. Ecol. 22: 3376–3390.

Drovetski, S. V. 2003. Plio-Pleistocene climatic oscilations, Holarctic biogeography and speciation in an avian subfamily. – J. Biogeogr. 30: 1173–1181.

Drummond, A. J., Suchard, M. A., Xie, D. and Rambaut, A. 2012. Bayesian phylogenetics with BEAUti and the BEAST 1.7. – Mol. Biol. Evol. 29: 1969–1973.

Dynesius, M. and Jansson, R. 2000. Evolutionary consequences of changes in species' geographical distributions driven by Milankovitch climate oscillations. – Proc. Natl Acad. Sci. USA 97: 9115–9120.

Excoffier, L. and Lischer, H. E. L. 2010. Arlequin suite ver 3.5: a new series of programs to perform population genetics analyses under Linux and Windows. – Mol. Ecol. Resour. 10: 564–567.

Fregin, S., Haase, M., Olsson, U. and Alstrom, P. 2012. Pitfalls in comparisons of genetic distances: a case study of the avian family Acrocephalidae. – Mol. Phylogenet. Evol. 62: 319–328.

Fu, Y. X. 1997. Statistical tests of neutrality of mutations against population growth, hitchhiking and background selection. – Genetics 147: 915–925.

García, J. T., Suárez, F., Garza, V., Calero-Riestra, M., Hernández, J. and Pérez-Tris, J. 2008. Genetic and phenotypic variation among geographically isolated populations of the globally threatened Dupont's lark *Chersophilus duponti*. – Mol. Phylogenet. Evol. 46: 237–251.

Gill, F. and Donsker, D. 2015. IOC World bird list v 5.1. – <www.worldbirdnames.org>.

Guillaumet, A., Pons, J. M., Godelle, B. and Crochet, P. A. 2006. History of the crested lark in the Mediterranean region as revealed by mtDNA sequences and morphology. – Mol. Phylogenet. Evol. 39: 645–656.

Guindon, S. and Gascuel, O. 2003. A simple, fast, and accurate algorithm to estimate large phylogenies by maximum likelihood. – Syst. Biol. 52: 696–704.

Guisan, A. and Thuiller, W. 2005. Predicting species distribution: offering more than simple habitat models. – Ecol. Lett. 8: 993–1009.

Hackett, S. J. 1996. Molecular phylogenetics and biogeography of tanagers in the genus *Ramphocelus* (Aves). – Mol. Phylogenet. Evol. 5: 368–382.

Haring, E., Gamauf, A. and Kryukov, A. 2007. Phylogeographic patterns in widespread Corvid birds. – Mol. Phylogenet. Evol. 45: 840–862.

Harrison, S. P., Yu, G., Takahara, H. and Prentice, I. C. 2001. Palaeovegetation – diversity of temperate plants in east Asia. – Nature 413: 129–130.

Hewitt, G. 2000. The genetic legacy of the Quaternary ice ages. – Nature 405: 907–913.

Hewitt, G. M. 1996. Some genetic consequences of ice ages, and their role in divergence and speciation. – Biol. J. Linn. Soc. 58: 247–276.

Hewitt, G. M. 2004. Genetic consequences of climatic oscillations in the Quaternary. – Phil. Trans. R. Soc. B 359: 183–195.

Hijmans, R. J., Cameron, S. E., Parra, J. L., Jones, P. G. and Jarvis, A. 2005. Very high resolution interpolated climate surfaces for global land areas. – Int. J. Climatol. 25: 1965–1978.

Hogner, S., Laskemoen, T., Lifjeld, J. T., Porkert, J., Kleven, O., Albayrak, T., Kabasakal, B. and Johnsen, A. 2012. Deep sympatric mitochondrial divergence without reproductive isolation in the common redstart *Phoenicurus phoenicurus*. – Ecol. Evol. 2: 2974–2988.

Hourlay, F., Libois, R., D'Amico, F., Sará, M., O'Halloran, J. and Michaux, J. R. 2008. Evidence of a highly complex phylogeographic structure on a specialist river bird species, the dipper (*Cinclus cinclus*). – Mol. Phylogenet. Evol. 49: 435–444.

Huang, Z. H., Liu, N. F., Liang, W., Zhang, Y. Y., Liao, X. J., Ruan, L. Z . and Yang, Z. S. 2010. Phylogeography of Chinese bamboo partridge, *Bambusicola thoracica thoracica* (Aves: Galliformes) in south China: inference from mitochondrial DNA control-region sequences. – Mol. Phylogenet. Evol. 56: 273–280.

Irwin, D. E., Rubtsov, A. S. and Panov, E. N. 2009. Mitochondrial introgression and replacement between yellowhammers (*Emberiza citrinella*) and pine buntings (*Emberiza leucocephalos*) (Aves: Passeriformes). – Biol. J. Linn. Soc. 98: 422–438.

Johnsen, A., Rindal, E., Ericson, P. G., Zuccon, D., Kerr, K. C., Stoeckle, M. Y. and Lifjeld, J. T. 2010. DNA barcoding of Scandinavian birds reveals divergent lineages in trans-Atlantic species. – J. Ornithol. 151: 565–578.

Johnson, K. P. and Sorenson, M. D. 1998. Comparing molecular evolution in two mitochondrial protein coding genes (cytochrome b and ND2) in the dabbling ducks (tribe Anatini). – Mol. Phylogenet. Evol. 10: 82–94.

Kimura, M. 1980. A simple method for estimating evolutionary rates of base substitutions through comparative studies of nucleotide-sequences. – J. Mol. Evol. 16: 111–120.

Klicka, J., Johnson, K. P. and Lanyon, S. M. 2000. New world nine-primaried oscine relationships: constructing a mitochondrial DNA framework. – Auk 117: 321–336.

Klicka, J., Spellman, G. M., Winker, K., Chua, V. and Smith, B. T. 2011. A phylogeographic and population genetic analysis of a widespread, sedentary North American bird: the hairy woodpecker (*Picoides villosus*). – Auk 128: 346–362.

Lerner, H. R. L., Meyer, M., James, H. F., Hofreiter, M. and Fleischer, R. C. 2011. Multilocus resolution of phylogeny and timescale in the extant adaptive radiation of Hawaiian honeycreepers. – Curr. Biol. 21: 1838–1844.

Li, S. H., Yeung, C. K. L., Feinstein, J., Han, L. X., Manh, H. L., Wang, C. X. and Ding, P. 2009. Sailing through the Late Pleistocene: unusual historical demography of an east Asian endemic, the Chinese hwamei (*Leucodioptron canorum canorum*), during the last glacial period. – Mol. Ecol. 18: 622–633.

Librado, P. and Rozas, J. 2009. DnaSP v5: a software for comprehensive analysis of DNA polymorphism data. – Bioinformatics 25: 1451–1452.

Lovette, I. J. 2004. Mitochondrial dating and mixed-support for the "2% rule" in birds. – Auk 121: 1–6.

Manthey, J. D., Klicka, J. and Spellman, G. M. 2011. Cryptic diversity in a widespread North American songbird: phylogeography of the brown creeper (*Certhia americana*). – Mol. Phylogenet. Evol. 58: 502–512.

Martinez-Meyer, E. and Peterson, A. T. 2006. Conservatism of ecological niche characteristics in North American plant species over the Pleistocene-to-Recent transition. – J. Biogeogr. 33: 1779–1789.

Ödeen, A. 2001. Loss and gain of sexual traits, radiation and convergent evolution in yellow wagtails (*Motacilla flava* L.). – PhD. thesis, Uppsala Univ.

Ödeen, A. and Alström, P. 2001. Evolution of secondary sexual traits in wagtails (genus *Motacilla*). – PhD thesis, Uppsala Univ.

Ödeen, A. and Björklund, M. 2003. Dynamics in the evolution of sexual traits: losses and gains, radiation and convergence in yellow wagtails (*Motacilla flava*). – Mol. Ecol. 12: 2113–2130.

Otto-Bliesner, B. L., Brady, E. C., Clauzet, G., Tomas, R., Levis, S. and Kothavala, Z. 2006. Last Glacial Maximum and Holocene climate in CCSM3. – J. Clim. 19: 2526–2544.

Pavlova, A., Zink, R. M., Drovetski, S. V., Red'kin, Y. and Rohwer, S. 2003. Phylogeographic patterns in *Motacilla flava* and *Motacilla citreola*: species limits and population history. – Auk 120: 744–758.

Pavlova, A., Zink, R. M., Rohwer, S., Koblik, E. A., Red'kin, Y. A., Fadeev, I. V. and Nesterov, E. V. 2005. Mitochondrial DNA and plumage evolution in the white wagtail *Motacilla alba*. – J. Avian Biol. 36: 322–336.

Pavlova, A., Rohwer, S., Drovetski, S. V. and Zink, R. M. 2006. Different post-pleistocene histories of Eurasian parids. – J. Hered. 97: 389–402.

Pearson, R. G., Raxworthy, C. J., Nakamura, M. and Peterson, A. T. 2007. Predicting species distributions from small numbers of occurrence records: a test case using cryptic geckos in Madagascar. – J. Biogeogr. 34: 102–117.

Peng, Y. Z., Yang, D. H. and Kuang, B. Y. 1987. The avifauna of Yunnan province. – Yunnan Sci. and Tech. Press.

Peterson, A. T., Soberon, J. and Sanchez-Cordero, V. 1999. Conservatism of ecological niches in evolutionary time. – Science 285: 1265–1267.

Phillips, S. J. and Dudik, M. 2008. Modeling of species distributions with Maxent: new extensions and a comprehensive evaluation. – Ecography 31: 161–175.

Pons, J. M., Olioso, G., Cruaud, C. and Fuchs, J. 2011. Phylogeography of the Eurasian green woodpecker (*Picus viridis*). – J. Biogeogr. 38: 311–325.

Posada, D. 2008. jModelTest: phylogenetic model averaging. – Mol. Biol. Evol. 25: 1253–1256.

Posada, D. and Buckley, T. R. 2004. Model selection and model averaging in phylogenetics: advantages of Akaike information criterion and Bayesian approaches over likelihood ratio tests. – Syst. Biol. 53: 793–808.

Qu, Y. H., Zhang, R. Y., Quan, Q., Song, G., Li, S. H. and Lei, F. M. 2012. Incomplete lineage sorting or secondary admixture: disentangling historical divergence from recent gene flow in the vinous-throated parrotbill (*Paradoxornis webbianus*). – Mol. Ecol. 21: 6117–6133.

Qu, Y. H., Ericson, P. G. P., Quan, Q., Song, G., Zhang, R. Y., Gao, B. and Lei, F. M. 2014. Long-term isolation and stability explain high genetic diversity in the eastern Himalaya. – Mol. Ecol. 23: 705–720.

Rambaut, A. and Drummond, A. J. 2007. Tracer v1.4. – <http://beast.bio.ed.ac.uk/Tracer>.

Rheindt, F. E. and Edwards, S. V. 2011. Genetic introgression: an integral but neglected component of speciation in birds. – Auk 128: 620–632.

Rogers, A. R. and Harpending, H. 1992. Population-growth makes waves in the distribution of pairwise genetic-differences. – Mol. Biol. Evol. 9: 552–569.

Ronquist, F. and Huelsenbeck, J. P. 2003. MrBayes 3: Bayesian phylogenetic inference under mixed models. – Bioinformatics 19: 1572–1574.

Ruokonen, M. and Kvist, L. 2002. Structure and evolution of the avian mitochondrial control region. – Mol. Phylogenet. Evol. 23: 422–432.

Saetre, G. P., Borge, T., Lindell, J., Moum, T., Primmer, C. R., Sheldon, B. C., Haavie, J., Johnsen, A. and Ellegren, H. 2001. Speciation, introgressive hybridization and nonlinear rate of molecular evolution in flycatchers. – Mol. Ecol. 10: 737–749.

Saitoh, T., Alström, P., Nishiumi, I., Shigeta, Y., Williams, D., Olsson, U. and Ueda, K. 2010. Old divergences in a boreal

bird supports long-term survival through the Ice Ages. – BMC Evol. Biol. 10: 35.
Smith, B. T., Escalante, P., Hernandez, B. B. E., Navarro-Sigueenza, A. G., Rohwer, S. and Klicka, J. 2011. The role of historical and contemporary processes on phylogeographic structure and genetic diversity in the northern cardinal, *Cardinalis cardinalis*. – BMC Evol. Biol. 11: 136.
Song, G., Qu, Y. H., Yin, Z. H., Li, S. H., Liu, N. F. and Lei, F. M. 2009. Phylogeography of the *Alcippe morrisonia* (Aves: Timaliidae): long population history beyond late Pleistocene glaciations. – BMC Evol. Biol. 9: 143.
Sorenson, M. D. and Quinn, T. W. 1998. Numts: a challenge for avian systematics and population biology. – Auk 115: 214–221.
Sorenson, M. D., Ast, J. C., Dimcheff, D. E., Yuri, T. and Mindell, D. P. 1999. Primers for a PCR-based approach to mitochondrial genome. – Mol. Phylogenet. Evol. 12: 105–144.
Stepanyan, L. S. 1990. Conspectus of the ornithological fauna of the USSR. – Nauka.
Stervander, M., Illera, J. C., Kvist, L., Barbosa, P., Keehnen, N. P., Pruisscher, P., Bensch, S. and Hansson, B. 2015. Disentangling the complex evolutionary history of the western Palearctic blue tits (*Cyanistes* spp.) – phylogenomic analyses suggest radiation by multiple colonization events and subsequent isolation. – Mol. Ecol. 24: 2477–2494.
Tajima, F. 1989. Statistical-method for testing the neutral mutation hypothesis by DNA polymorphism. – Genetics 123: 585–595.
Tamura, K., Peterson, D., Peterson, N., Stecher, G., Nei, M. and Kumar, S. 2011. MEGA5: molecular evolutionary genetics analysis using maximum likelihood, evolutionary distance, and maximum parsimony methods. – Mol. Biol. Evol. 28: 2731–2739.
Tarr, C. L. 1995. Primers for amplification and determination of mitochondrial control-region sequences in oscine passerines. – Mol. Ecol. 4: 527–529.
Thompson, J. D., Gibson, T. J., Plewniak, F., Jeanmougin, F. and Higgins, D. G. 1997. The ClustalX windows interface: flexible strategies for multiple sequence alignment aided by quality analysis tools. – Nucleic Acids Res. 25: 4876–4882.
van Els, P., Cicero, C. and Klicka, J. 2012. High latitudes and high genetic diversity: phylogeography of a widespread boreal bird, the gray jay (*Perisoreus canadensis*). – Mol. Phylogenet. Evol. 63: 456–465.
Voelker, G. 2002. Systematics and historical biogeography of wagtails: dispersal versus vicariance revisited. – Condor 104: 725–739.
Walstrom, V. W., Klicka, J. and Spellman, G. M. 2012. Speciation in the white-breasted nuthatch (*Sitta carolinensis*): a multilocus perspective. – Mol. Ecol. 21: 907–920.

Supplementary material (Appendix JAV-00826 at <www.avianbiology.org/appendix/jav-00826>). Appendix 1–3.

Wang, W. J., McKay, B. D., Dai, C. Y., Zhao, N., Zhang, R. Y., Qu, Y. H., Song, G., Li, S. H., Liang, W., Yang, X. J., Pasquet, E. and Lei, F. M. 2013. Glacial expansion and diversification of an east Asian montane bird, the green-backed tit (*Parus monticolus*). – J. Biogeogr. 40: 1156–1169.
Wang, W. J., Dai, C. Y., Alström, P., Zhang, C. L., Qu, Y. H., Li, S. H., Yang, X. J., Zhao, N., Song, G. and Lei, F. M. 2014. Past hybridization between two east Asian long-tailed tits (*Aegithalos bonvaloti* and *A. fuliginosus*). – Front. Zool. 11: 40.
Warren, D. L., Glor, R. E. and Turelli, M. 2010. ENMTools: a toolbox for comparative studies of environmental niche models. – Ecography 33: 607–611.
Weaver, A. J., Eby, M., Augustus, F. F. and Wiebe, E. C. 1998. Simulated influence of carbon dioxide, orbital forcing and ice sheets on the climate of the Last Glacial Maximum. – Nature 394: 847–853.
Webb, W. C., Marzluff, J. M. and Omland, K. E. 2011. Random interbreeding between cryptic lineages of the common raven: evidence for speciation in reverse. – Mol. Ecol. 20: 2390–2402.
Weir, J. T. and Schluter, D. 2004. Ice sheets promote speciation in boreal birds. – Proc. R. Soc. B 271: 1881–1887.
Weir, J. T. and Schluter, D. 2008. Calibrating the avian molecular clock. – Mol. Ecol. 17: 2321–2328.
Williams, D., Dunkerley, D., DeDeckker, P., Kershaw, P. and Chappell, M. 1998. Quaternary environments. – Arnold.
yWorks 2012. – < http://www.yworks.com/ >.
Zhao, N., Dai, C. Y., Wang, W. J., Zhang, R. Y., Qu, Y. H., Song, G., Chen, K., Yang, X. J., Zou, F. S. and Lei, F. M. 2012. Pleistocene climate changes shaped the divergence and demography of Asian populations of the great tit *Parus major*: evidence from phylogeographic analysis and ecological niche models. – J. Avian Biol. 43: 297–310.
Zhao, Z. J. 2001. The avifauna of China. – Jilin Sci. and Tech. Press.
Zink, R. M. and Blackwell, R. C. 1998. Molecular systematics and biogeography of aridland gnatcatchers (genus *Polioptila*) and evidence supporting species status of the California gnatcatcher (*Polioptila californica*). – Mol. Phylogenet. Evol. 9: 26–32.
Zink, R. M. and Weckstein, J. D. 2003. Recent evolutionary history of the fox sparrows (genus: *Passerella*). – Auk 120: 522–527.
Zink, R. M., Drovetski, S. V. and Rohwer, S. 2006. Selective neutrality of mitochondrial ND2 sequences, phylogeography and species limits in *Sitta europaea*. – Mol. Phylogenet. Evol. 40: 679–686.
Zink, R. M., Pavlova, A., Drovetski, S. and Rohwer, S. 2008. Mitochondrial phylogeographies of five widespread Eurasian bird species. – J. Ornithol. 149: 399–413.